

## Design and development of cyclic hydrostatic stress-generating machine for articular cartilage chondrocytes

GARIMA SHARMA\*, R. K. SAXENA AND SOHIT KAROL

Center for Biomedical Engineering, Indian Institute of Technology Delhi, New Delhi 110 016, India.  
email: sharmagarima\_s@rediffmail.com; Phone: 91-11-26596153.

Received on September 26, 2005, Revised on March 8, 2006, and March 21, 2006.

### Abstract

Mechanical stimulation of articular cartilage at certain range of loading plays important role in the maintenance of tissue under normal physiological conditions, whereas abnormal forces might lead to its degeneration and pathological condition like osteoarthritis. With an objective to elucidate the role of mechanical stresses and their molecular/cellular correlations on cartilage metabolism, we have designed and developed a custom-made machine for generating hydrostatic load (cyclic and static) on articular cartilage chondrocytes cultured in alginate matrix. The main machine frame consists of three functional units: sample holding unit (to keep the cell sample), loading unit (to generate the load) and control-cum-driving unit (to operate and control the load patterns). The working mechanism of cyclic hydrostatic stress-generating machine is based on cam/follower arrangement and controlled by a two-phase stepper motor. The machine has been developed and used for generating physiological cyclic as well as static pressure ranging from 1–3 MPa under wide frequencies (0.33–3 Hz) at chondrocytes laden alginate beads. Efficacy and accuracy of machine has been evaluated by studying load-related alterations in morphological properties of goat chondrocytes encapsulated in alginate beads.

**Keywords:** Articular cartilage, cyclic loading, alginate, hydrostatic pressure, cam.

### 1. Introduction

Articular cartilage is a specialised type of connective tissue, which forms the load-bearing surface of the subchondral bones in a diarthroidal joint. It is subjected to very high compressive and shearing forces, which can rise up to 100–200 atm (10–20 MPa) within milliseconds during normal joint activities like walking and jumping [1, 2]. The extracellular matrix and cells provide enormous weight-resisting property to healthy articular cartilage. The chondrocytes are able to sense and respond to the mechanical stimulations on cartilage tissue through an intracellular signalling process known as mechanotransduction. This is evident by the altering metabolic and material properties of cartilage during compressive and shear loading of the tissue and under degenerative joint conditions like arthritis [3–8]. However, the mechanism by which chondrocytes recognize these physical signals and translate them into molecular and biochemical responses is not yet completely understood. Several *in vitro* studies of cartilage physical stimulations have been carried out utilizing various mechanical stimuli such as dynamic or static compression of explants [9–15], fluid-induced shear stress [16–18] and gas-pressurized chambers on isolated chondrocytes in

\*Author for correspondence.

monolayers [19–21]. The loads generated in the case of shear stress and gas chamber remain quite low considering the large forces acting on human knee or hip joint and hence do not provide realistic assessments [22]. The hydrostatic pressure is believed to represent one of the most important physical forces acting in cartilage during deformation of cartilage [23] and changes momentarily during loading [24]. Recent studies have shown that hydrostatic pressure application on articular cartilage chondrocyte alters their synthetic capacity depending upon the load frequency, strength and duration [25–29]. However, most of these studies have been carried out on isolated chondrocyte monolayer culture or cartilage explants and employ the gas phase. The present study was carried out with the objective of developing a mechanical compression-based loading system for application of purely hydrostatic cyclic and static pressure (with no gas phase present) on articular chondrocytes seeded in 3D matrix (alginate) over wide range of magnitude and frequencies. The isolated chondrocytes cultured in alginate beads synthesize cartilage-specific matrix and form a tissue similar to that of native cartilage both functionally and structurally [30]. The mechanical stimulations of chondrocytes in such conditions can provide true insight into cellular-level functions that are difficult to measure *in vivo* or in cartilage explants.

## 2. Materials and methods

### 2.1. Isolation of articular cartilage chondrocytes and encapsulation in alginate

Articular cartilage samples were collected aseptically from the femopatellar joint of young goat (2–3 months age, mean weight  $20 \pm 1.5$  kg) and chondrocytes were isolated by enzymatic digestion using papain, hyaluronidase and type II collagenase [31]. The isolated viable chondrocytes were encapsulated in 3% alginate by syringe extrusion method at final concentration of  $2 \times 10^6$  cell/ml [32]. The chondrocyte-laden beads were kept in Dulbecco's modified eagle medium (DMEM) containing 10% FBS in 5% CO<sub>2</sub> at 37°C and replaced with fresh medium every alternate day.

### 2.2. Design requirements of 'cyclic hydrostatic stress generating machine'

The alginate-encapsulated articular cartilage chondrocytes are required to be subjected to cyclic and static pressure at physiological range (1–5 MPa). The range of pressure was chosen keeping in view the surface area of joint and weight of animal. The cartilage surface area is approximately 2 cm<sup>2</sup> and mean body weight of animal is 20 kg, hence the force at the surface would be  $20 \times 9.8 = 196$  N which gives rise to hydrostatic pressure of approximately (at each articular joint surface out of 4)  $196/2 \times 10^{-4} \times 4 = 2,45,000$  N/m<sup>2</sup> or 0.24 MPa. We approach to design a cyclic hydrostatic loading machine which is able to produce pressure regimen of 10–15 (up to 3.6 MPa) times of the average stress at the joint surface over a wide range of frequencies (0.3–3 Hz) for varying periods (4–24 hours). The cell sample-holding unit should have volume of approximately 5–7 cm<sup>3</sup>. It should be detachable from main assembly and fabricated of sterilizable and noncorrosive material. The machine should have a loading mechanism to be operated and controlled by stepper motor for application of desired compressive load on cells which can be changed as per the mechanical loading protocol. The loading machine was to be mounted on a sturdy and

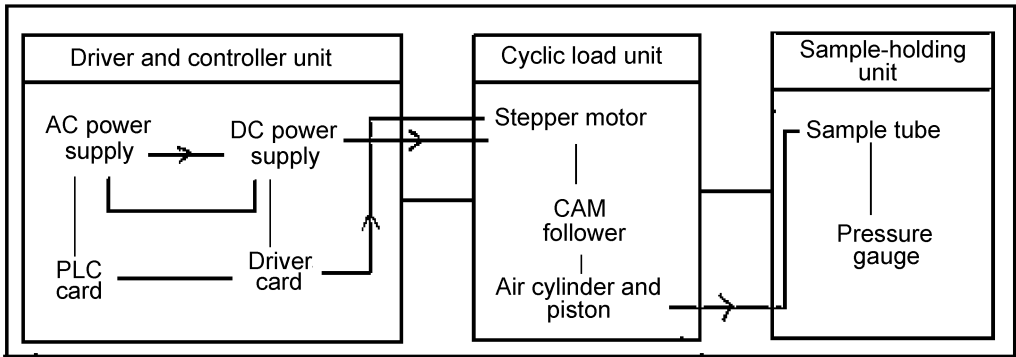


FIG. 1. Block diagram showing various units of 'cyclic hydrostatic stress-generating machine'.

vibration-free frame capable of withstanding high dynamic load during the course of experiment.

### 2.3. Principle of 'cyclic hydrostatic stress-generating machine'

The basic mechanism of design involves entrapping an air column above the medium containing the cells in alginate beads, and compressing and decompressing the air thus applying hydrostatic pressure of the air column on the medium and the cells by changing its length. As the air column was directly above the medium surface, and leakages from any susceptible points were prevented, it is assumed that the entire pressure got transmitted to the medium and subsequently onto chondrocyte cells. The hydrostatic pressure at a given depth in a static liquid is the result of the weight of the liquid acting on a unit area at that depth plus any pressure acting on the surface of the liquid.

The entire frame of 'cyclic hydrostatic stress-generating machine' is designed in three functional units: cell sample-holding unit, loading unit and driver-cum-controller unit (Fig. 1). Details of various parts of the units and their functionality are described in the later section.

### 2.4. Mechanism of cyclic hydrostatic stress-generating machine

Two separate steel cylinders, one as sample-holding unit, carrying chondrocyte-laden alginate beads in culture medium and the other air cylinder having an air column inside, were fixed together with leak proof pressure joints, flanges and bolts. An airtight stainless steel piston inside the air cylinder is used to compress the air entrapped above the surface of the medium. The piston was connected to the cam/roller follower assembly with the help of a forked key. The shape of cam or cam profile is the most critical part of the machine for generating desired cyclic load patterns on chondrocytes. The cam was attached to the shaft of the stepper motor and as it rotates, the follower oscillates by simple harmonic motion. The axial movements of piston compress the air column and generate cyclic hydrostatic pressure on the cells in accordance to cam profile.

### 3. Design details of ‘Cyclic hydrostatic stress-generating machine’

#### 3.1. The sample-holding unit

The sample-holding tube is a stainless steel cylinder which bears the alginate beads carrying chondrocytes in culture medium. The optimal volume of the unit is kept at 7 ml to accommodate approximately 100 beads ( $\sim 1 \times 10^6$  cells) in 5-ml culture medium. The internal diameter of the cylinder is 10 mm keeping in view the dimensions of air cylinder and piston. The length of the cylinder is calculated from the volume and radius of the cylinder ( $V = \pi r^2 h$ ) and found to be 85 mm. The top and base plates of the sample-holding tube are made up of stainless steel ( $\phi$  139 mm). The sample-holding unit was attached to air cylinder via top plate and to the main assembly via bottom plate with the help of 4 screws. A hole was drilled in the bottom of the sample-holding tube to accommodate a pressure gauge (50 kg/cm<sup>2</sup>). A sectional view of the sample-holding unit (A–A') is shown in Fig. 2.

#### 3.2. The loading unit

The loading unit is the heart of the machine which generates and controls the varying loading patterns on cells. It consists of four main components: air cylinder, piston, cam/follower assembly and stepper motor.

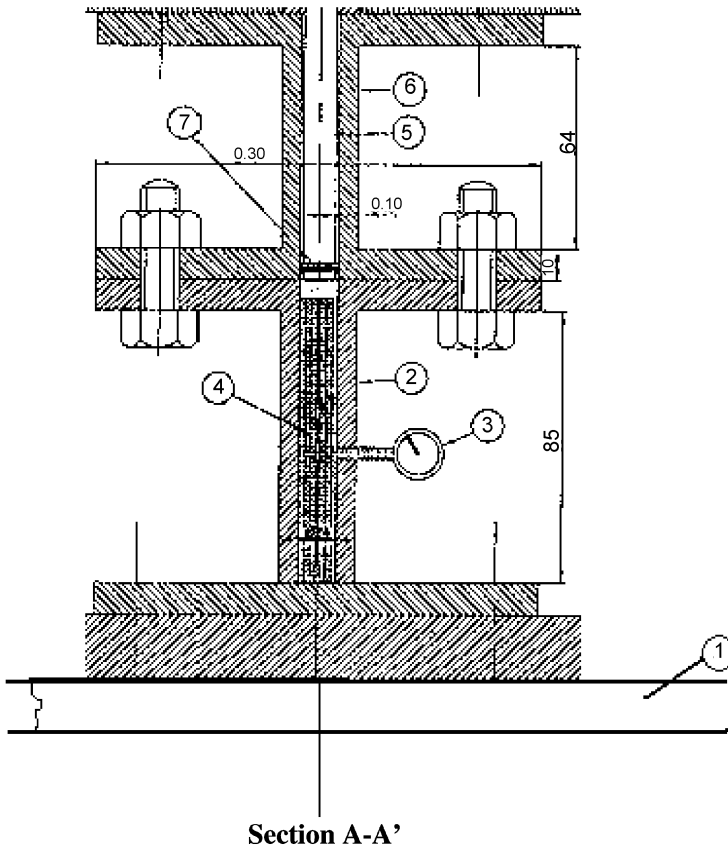
**Air cylinder:** The air cylinder is made up of stainless steel and has inner diameter equal to diameter of piston and sample-holding unit (10 mm) as to join them completely to make system leak proof. The air cylinder is fixed to the sample-holding tube via its bottom plate (Fig. 2).

**Piston:** A vertical motion piston was fabricated with high-grade stainless steel to minimize corrosion and alteration in dimensions during continuous movement along the walls of air cylinder. The diameter of the piston is 10 mm to move smoothly in the air cylinder. The length of the piston ( $L$ ) is calculated using Boyle's law. At 37°C temperature and 0.1 MPa atmospheric pressure, the initial air column length [ $l_1$ ] at the top position of piston is 64 mm (length of air cylinder); therefore, the final length of air column [ $l_2$ ] for getting maximum pressure of 3.6 MPa can be calculated as:

$$l_2 = P_1 l_1 / P_2, \quad l_2 = 0.1 \times 64 / 3.6 = 1.78 \text{ mm.}$$

The length of the piston  $L = l_1 + l_2 = (64 + 1.78) = 65.78$  mm, the final length was kept twice that of  $L$  for getting hold and attachment with the other loading components like forked key, roller follower and cam. The height of mounting of stepper motor and length of forked key were also considered in this. The final length of piston is kept 135 mm (Fig. 3).

At the posterior end of the piston two silicon rubber o-rings ( $\phi$  8mm) were accommodated for preventing any leakage of pressure. A brass bush was designed ( $\phi$  10 mm) and inserted at the anterior end of the piston where it enters the air cylinder. A linear motion bearing is used between piston and bush to minimize friction during axial motion. The piston was attached to roller follower using a mild steel forked key (35 mm length) which is fixed in bracket eye.



Section A-A'

FIG. 2. Sectional view of the sample-holding unit of 'cyclic hydrostatic stress-generating machine' showing attachment with air cylinder and main assembly. 1. Base plate, 2. Sample-holding tube, 3. Pressure gauge, 4. Cells in medium, 5. Air piston, 6. Air cylinder and 7. O-rings.

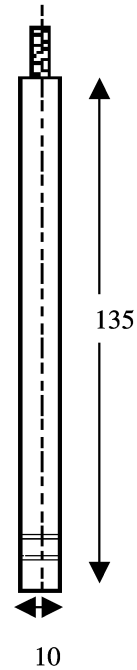


FIG. 3. Schematic drawing of the piston.

**Cam/roller follower:** For obtaining the desired pressure profile on the cells, cams of various sizes and angles are designed and manufactured. The designing of the cam profile is the most critical part of the machine as it controls the load generated on the chondrocyte-laden beads. A radial cam was designed for obtaining a cyclic load pattern ranging from 0.2 to 5 MPa. The diameter of the camshaft is equal to the shaft of the stepper motor (14 mm). The center of the follower is the trace point of the cam. The diameter of the base circle is kept 5–7 mm greater than the camshaft diameter and is approximately 21 mm. The displacement of the follower was chosen to be in simple harmonic motion. The details about the cam profile and calculation of cyclic load obtained are discussed later.

A spring was used ( $n = 0.3$ ) to keep the roller follower in contact with the cam. A standard diameter of spring wire SWG 8 ( $d = 1.54$  mm) was used. The mean diameter of the spring coil is 15.79 mm and the number of turns is 13. The free length of the spring is 78 mm. Supporting frames of the machine and other parts like base plates, angle plates (for

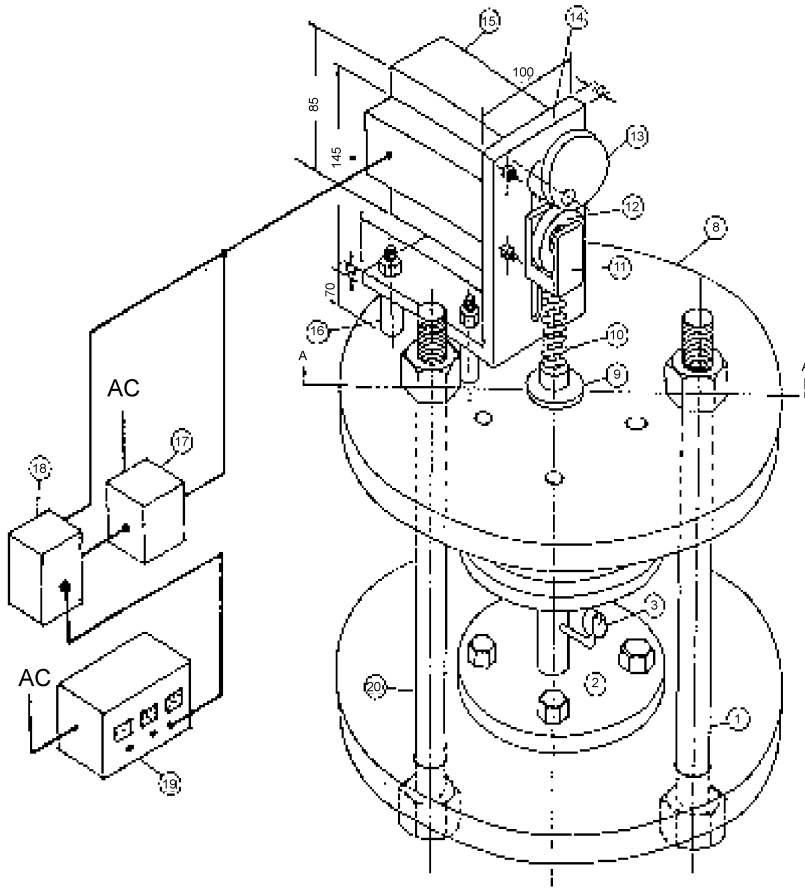


FIG. 4. Isometric view of Cyclic hydrostatic stress-generating machine. 1. High-tensile bolts, 2. Sample tube, 3. Pressure gauge, (4, 5, 6, 7: Cell sample, Piston, Air cylinder and O-rings shown in Fig. 2), 8. Upper plate, 9. Brass bush, 10. Spring, 11. Forked key, 12. Roller bearing, 13. Cam, 14. Angle plate, 15. Stepper motor, 16. Spacers, 17. Controller card, 18. Driver card, and 19. Power supply.

mounting stepper motor), pillar bolts, O-rings were commercially available and were used without any further machining. The use of high-tensile-strength components provides sturdiness to the machine during higher loading conditions and prevents changes in dimensions and functioning of the machine.

**Stepper motor:** A mycom 2-phase stepper motor of 44 kg cm holding torque with 200 steps per revolution is used. The motor is mounted on the top plate of the assembly with the help of L-shaped steel angle plates.

### 3.3. Driver and controller unit

The driver and controller unit consist of a driver card used with stepper motor (mycom 2-phase stepper drive) and a Fatek S-Series 8-input, 6-output PLC. The driver and controller

were installed with motor and adjusted to provide 40 rpm (0.66 Hz) to shaft of motor. The power supply was given via a multi-output DC power supply system. The isometric view of the 'cyclic hydrostatic stress machine' is shown in Fig. 4.

### 3.4. Cam profile and its relation with generation of cyclic loading

A radial cam of 31-mm lift was designed. It is driven clockwise by stepper motor at a uniform speed of 40 rpm and the follower motion will be according to the shape of the cam. The follower moves with simple harmonic motion and the following load pattern was adopted during one rotation of cam:

Follower rises from 0 to 30 mm for the first 120° of cam rotation in the clockwise direction

Follower dwells for the next 60° of cam rotation

Follower falls back to its initial position during the next 90° of cam rotation

Follower dwells for the next 90° of cam rotation.

The velocity of the follower is 0 at the beginning and at the end of the stroke and increases gradually to a maximum at mid-stroke and remains constant for 0.3 s.

The total angular distance for one complete rotation of cam (360°) can be subdivided into 12 equal divisions. As the cam rotates with a uniform velocity of 40 rpm, the total time taken in one complete revolution is 1.5 s and for each 30° angular displacement, the time taken by cam would be 0.125 s. The displacement diagram of the cam at various angles is shown as Fig. 5. The linear distance of cam during pressure angles was measured and is shown in Fig. 6.

### 3.5. Calculation of pressure generated at chondrocytes in alginate beads by cam/follower movement

Since the follower moves with SHM, the velocity diagram consists of a sine curve and the acceleration diagram is a cosine curve. The weight of the follower is 0.226 kg and the force generated by the piston at the given point of the cam is calculated as given in appendix. The pressure can be calculated by dividing the force with the surface area of the piston ( $A = 2\pi r^2 + 2\pi rh$ , where  $r = 5$  mm and  $h = 135$  mm). The displacement, velocity, and acceleration of follower with cam rotation and subsequent pressure generated is calculated at various angles and the load profile of 31 mm cam in one complete rotation is shown in Fig. 7.

## 4. Mechanical stimulation studies on chondrocytes using 'Cyclic hydrostatic stress-generating machine'

The finally developed machine has been tested for its functioning and accuracy on goat articular cartilage cells which have been encapsulated in alginate bead as described previously. Three sets of experiments were carried out on chondrocytes with both the cams at static and cyclic modes (0.66 Hz) for 4 h.

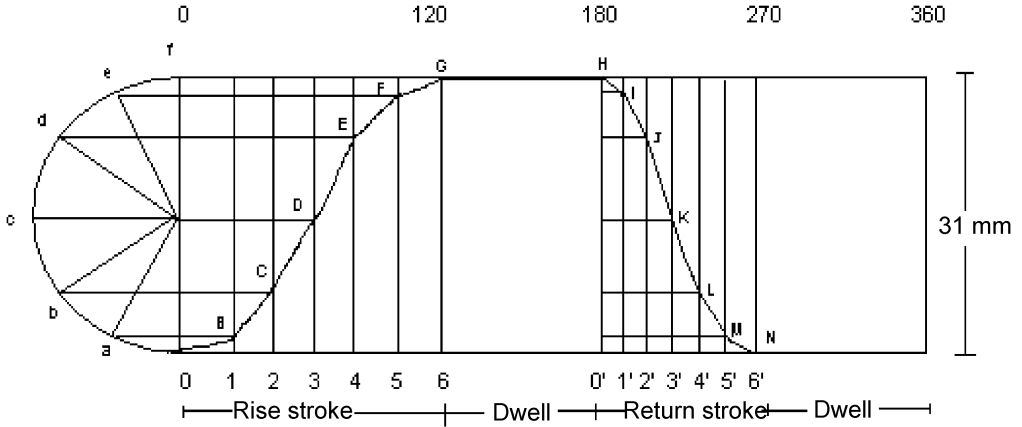


FIG. 5. The displacement diagram of the cam of 31-mm stroke.

4.1. Application of mechanical pressure on chondrocytes

Ten alginate beads (~25,000 cells/bead) were placed in pre-sterilized sample-holding tube of machine in 5 ml of culture medium and on top of it 2 ml of nonreactive, nonmiscible, high-density liquid paraffin oil layer was put for uniform loading. First, the 23-mm lift cam was fixed in the shaft of stepper motor and all other parts (sample-holding tube, piston, o-rings, etc.) were assembled firmly as per the design. The stepper motor driver card was given  $23 \pm 0.5$  V power via DC power supply and control card was attached to AC power. The controls were prepared in similar manner from the same batch of chondrocytes and maintained under standard cell culture conditions without load. In a similar manner, 31-mm cam was used. Both the cams were also used for providing static pressure by switching off the power of motor at a particular pressure angle of cam. At the end of loading experiments, loaded and unloaded beads were washed with phosphate buffer saline (pH 7.4) and were prepared for transmission electron microscopy for studying any load-related alterations in the ultrastructure and morphology of cells.

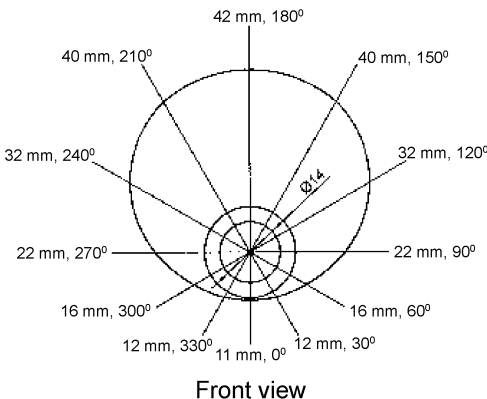


FIG. 6. Front view of a cam (lift 31 mm).

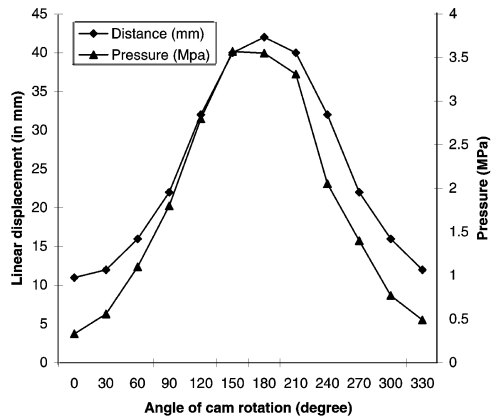


FIG. 7. Load profile of cam with 31-mm lift during one rotation.



#### 4.2. Transmission electron microscopy (TEM) analysis of chondrocytes in alginate

For morphological analysis by TEM, two alginate beads from each experiment were fixed at 4°C in 2.5% glutaraldehyde, rinsed overnight in 0.1 M cacodylate buffer and post-fixed for 4–5 h in 1% OsO<sub>4</sub>, dehydrated in a graded series of ethanol and embedded in Epon–Araldite [33]. Ultrathin sections were cut, stained with uranyl acetate and lead citrate and photographed with a Philips CM 10 electron microscope at the Department of Anatomy, All India Institute of Medical Sciences (AIIMS), New Delhi, India.

### 5. Results

A series of experiments were performed to validate the machine with cams of 31- and 23-mm lift which produce peak pressures of 24 and 12 kg/cm<sup>2</sup>, respectively, as measured by pressure gauge corresponding to 2.4 and 1.2 MPa. The cyclic loading mechanism provided the uniaxial compressive hydrostatic pressure to alginate seeded chondrocytes in reproducible manner over longer periods (up to 12 h) without any deterioration of the quality of signal. Figure 8(i) shows the photograph of the finally developed piston along with the roller, spring and forked key and Fig. 8(ii) the cam of 31- and 23-mm strokes. The complete assembly of the ‘cyclic hydrostatic stress-generating machine’ along with its functional units is shown in Fig. 8(iii).

#### 5.1. Transmission electron microscopy of chondrocytes at loading conditions

Representative images of chondrocytes under cyclic and static load of 1.2 and 2.4 MPa along with unloaded cells are shown in Fig. 9. Figure 9(a) shows an unloaded cell, round in shape, appears healthy, has continuous cell membrane and large round nucleus with rim of pericellular matrix around the cells. Also little ground matrix of proteoglycan granules and collagen fibrils is seen. Loading of chondrocytes at cyclic and static modes resulted in cell deformation from spherical to ellipsoidal morphology in a load-dependent manner. The cell deformation can be characterized grossly by a reduction in  $x/y$  ratio of cell, where  $x$  is horizontal diameter and  $y$  is the vertical diameter of chondrocyte. Figure 9(b) and (c) show the presence of abundant ground matrix of collagen fibrils and proteoglycan granules and thick pericellular matrix around cell during cyclic loads of 1.2 and 2.4 MPa, respectively. The presence of rich cell-matrix interaction and a well-characterized nucleus is also evident at cyclic loads.

The static load of 1.2 and 2.4 MPa also resulted in decreased  $x:y$  ratio in comparison to unloaded cells. However, almost negligible pericellular matrix and very less ground matrix was observed during static load 1.2 MPa which becomes almost absent at higher static load (2.4 MPa). Also, no significant cell–extracellular matrix attachment sites were observed at low and high static loads (Fig. 9(d) and (e)). The TEM pictures of chondrocytes at static load of 2.4 MPa show clearly disintegrating cell membrane, fragmented, irregular nucleus and presence of large vacuoles (Fig. 9(e)). All these ultrastructural features of cells indicate towards the static load-mediated damage to chondrocytes, which might result in degeneration of cell matrix also.

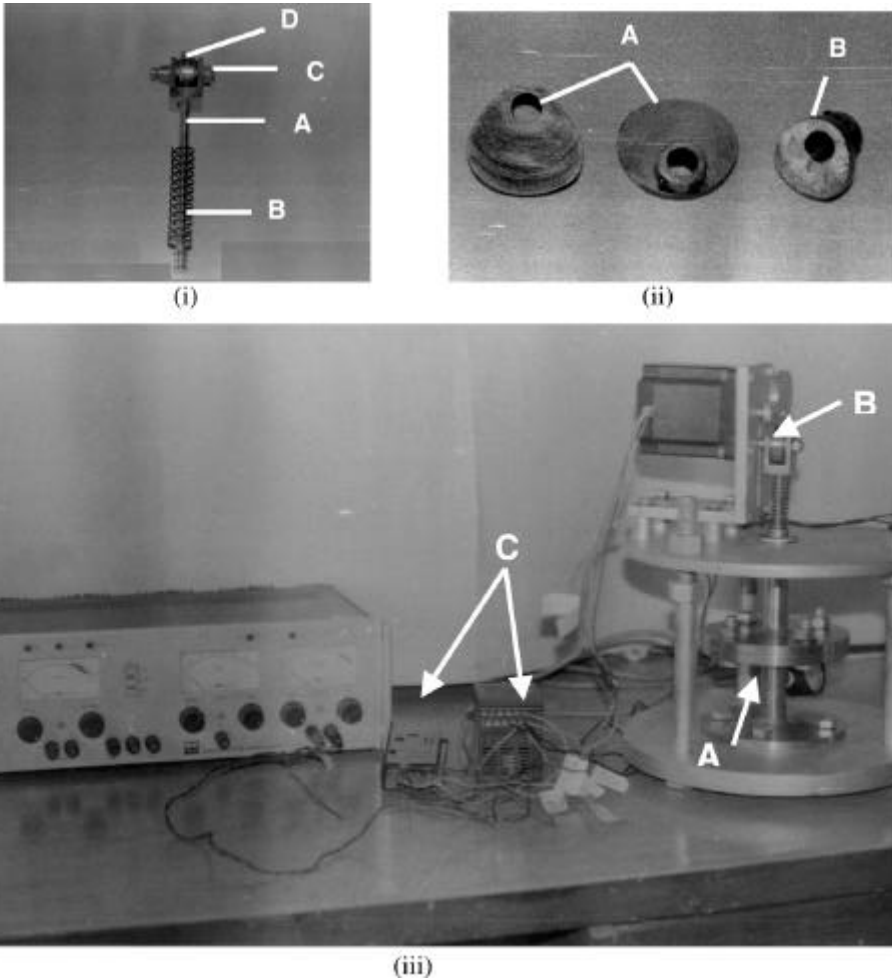


FIG. 8. (i) Photograph of the A. piston B. spring C. forked key D. roller, (ii) Cams of A. 31 mm and B. 23 mm stroke and (iii) complete assembly of 'cyclic hydrostatic stress-generating machine' showing A. sample-holding unit B. loading unit and C. driver-cum-controller unit.

## 6. Conclusion

A chondrocyte cyclic hydrostatic stress-generating machine was developed for application of cyclic pressure with high precision and repeatability on cartilage cells cultured in alginate matrix. Goat articular cartilage from small animal (2–3 months) was used as cell source as adult animal cartilage showed occasional degeneration and fibrillation of tissue. One of the novel features of the present *in vitro* loading machine is its capability to create both static and cyclic load thus making possible to study the various loading patterns in cyclic and static load or a combination of both. This is an important aspect of cartilage metabolism as cyclic loading has been suggested to have beneficial effect on cartilage health and matrix properties, whereas the reverse has been found for continuous loading [34]. In

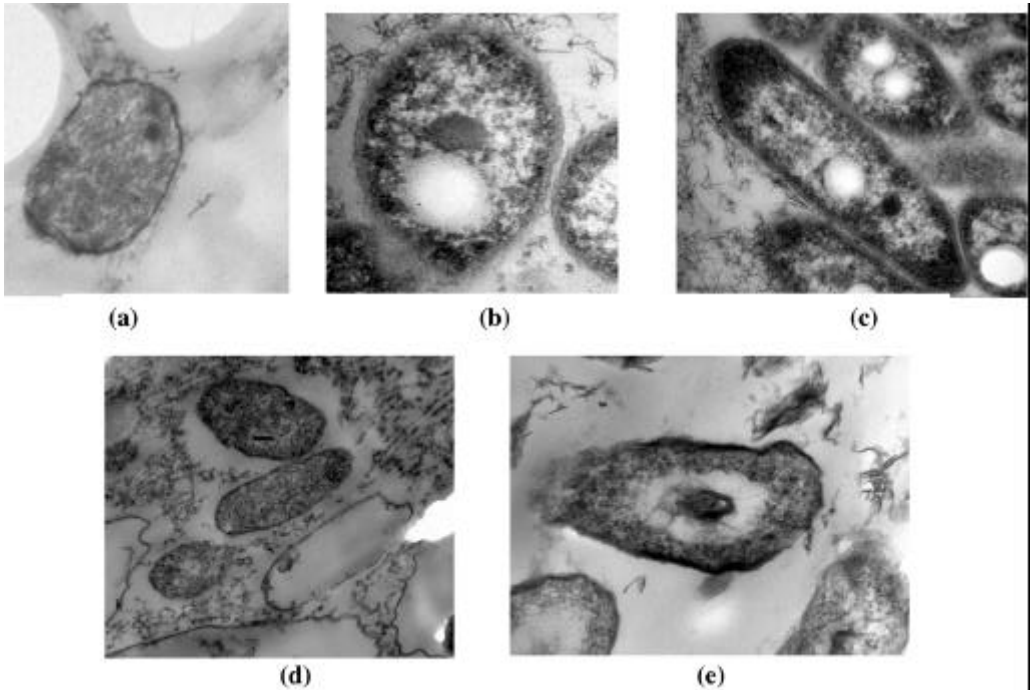


FIG. 9(a). TEM photographs of chondrocyte within alginate section, (a) cell without load, (b) and (c) cells at cyclic loads 1.2 and 2.4 MPa, respectively, and (d) and (e) cells at 1.2 and 2.4 MPa static load, respectively, 7200 $\times$ , bar = 1.5  $\mu$ m.

our initial study with this machine we also found improved proteoglycan and collagen content in chondrocytes under cyclic loading (data not shown). Here, we have investigated and presented the results of load-related alterations in morphological properties of cells. The increased cellular and matrix content, their interactions, and cell ultrastructural features have shown that cyclic pressure indeed has a positive effect on chondrocyte metabolism. In the case of static load, the TEM data has shown load-mediated damage to cell and its contents.

The design of the cam-operated system provides the potential to obtain very large hydrostatic pressure by changing the cam profile and pressure angles. The design of the system also provides the flexibility to increase or decrease the load just by changing the length of air piston or weight of follower. The electronically controlled driver system of machine provides a wide range of frequencies during cyclic load (0.33–3 Hz). Also the machine can be controlled further with computer using custom-made program or MATLAB.

Another unique feature of the machine is that it can be used for application of subambient pressure on the chondrocytes (by changing the direction of cam motion), i.e. pressure less than the atmospheric pressure. It has got a very important application as it has been recently discovered that during cyclic compressive loading of the joint, an intermittent negative pressure (vacuum) is created within the extracellular matrix of articular cartilage [35] and this pressure has a stimulatory effect on the metabolism of chondrocytes. Thus the machine may be used for visualizing and studying the negative pressure stimulation-related changes

in cartilage and their role in regeneration of the tissue in degenerative joint diseases like osteoarthritis and allied conditions.

The data obtained from the mechanical stimulation studies is informative for establishing the phenomenon of cartilage degeneration and regeneration. We believe that the machine we have designed and developed will be of great potential to form a composite picture about the physical regulation of cartilage in normal and pathological conditions as well as in cartilage engineering.

## References

1. W. A. Hodge, R. S. Fijan, K. L. Carlson, R. G. Burgers, W. H. Harris, and R. W. Mann, Contact pressure in the human hip joint measured *in vivo*, *Proc. Natn. Acad. Sci. USA*, **83**, 2879–2883 (1986).
2. A. Afoke, W. C. Hudson, and P. D. Byers, Pressure measurement in the human hip joint using Fuji film, In *Methods in cartilage research* (A. Marudodas and K. Kuettner, eds), Academic Press, pp. 281–287 (1991).
3. M. J. Palmoski, E. Perricone, and K. D. Brandt, Development of reversal of a proteoglycan aggregation defect in normal canine knee joint after immobilization, *Arthritis Rheum.*, **22**, 508–517 (1979).
4. I. Kiviranta, M. Tammi, J. Jurvelin, A. M. Saamanen, and H. J. Helminen, Moderate running exercise augments glycosaminoglycans and thickness of articular cartilage in the knee joints of young beagle dogs, *J. Orthop. Res.*, **6**, 188–195 (1988).
5. I. Kiviranta, M. Tammi, J. Jurvelin, J. Arokoski, A. M. Saamanen and H. J. Helminen, Articular cartilage thickness and glucosaminoglycal distribution in the canine knee joint after strenuous running exercise, *Clin. Orthop.*, **283**, 302–308 (1992).
6. J. Jurvelin, I. Kiviranta, A. M. Saamanen, M. Tammi and H. J. Helminen, Indentation stiffness of young canine knee articular cartilage: Influence of strenuous joint loading, *J. Biomech.*, **23**, 1239–1246 (1990).
7. E. L. Radin, R. B. Martin, D. B. Burr, B. Caterson, R. D. Boyd, and C. Goodwin, Effects of mechanical loadings on the tissues of rabbit knee, *J. Orthop. Res.*, **2**, 221–234 (1984).
8. R. D. Slowman, and K. D. Brandt, Composition and glycosaminoglycan metabolism of articular cartilage from habitually loaded and habitually unloaded sites, *Arthritis Rheum.*, **29**, 88–94 (1986).
9. P. A. Torzilli, R. Grigiene, C. Huang, S. M. Friedman, S. B. Doty, A. L. Boskey, and G. Lust, Characterization of cartilage metabolic response to static and dynamic stress using a mechanical explant testing system, *J. Biomech.*, **30**, 1–9 (1997).
10. J. Steinmeyer, A computer controlled mechanical culture system for biological testings of articular cartilage explants, *J. Biomech.*, **30**, 841–845 (1997).
11. K. M. Clements, Z. C. Bee, G. V. Crossingham, M. A. Adams, and M. Sharif, How severe must repetitive loading be to kill chondrocytes in articular cartilage?, *Osteoarthritis Cartilage*, **9**, 499–507 (2001).
12. D. D. D’Lima, S. Hashimoto, P. C. Chen, C. W. Colwell, and M. K. Lotz, Human chondrocytes apoptosis in response to mechanical injury, *Osteoarthritis Cartilage*, **8**, 712–719 (2001).
13. E. Lucchinetti, C. S. Adams and W. E. Horton Jr, Cartilage viability after repetitive loading: a preliminary report, *Osteoarthritis Cartilage*, **10**, 71–81 (2002).
14. B. Kurz, M. Jin, P. Patwari, D. M. Cheng, M. W. Lark, and A. J. Grodzinsky, Biosynthetic response and mechanical properties of articular cartilage after injurious compression, *J. Orthop. Res.*, **19**, 1140–1146 (2001).
15. R. K. Saxena, K. B. Sahay, and S. K. Guha, Biomechanical, biochemical and morphological correlates of bovine knee joint articular cartilage, *Instn Engrs (I)*, **75**, 8–16 (1994).
16. R. L. Smith, B. S. Donlon, M. K. Gupta, M. Mohtai, P. Das, D. R. Carter, J. Cooke, G. Gibbons, N. Hutchinson, and D. J. Schurman, Effects of fluid induced shear on articular chondrocytes morphology and metabolism *in vitro*, *J. Orthop. Res.*, **13**, 824–831 (1995).

17. M. T. Dewitt, C. J. Handley, B. W. Oakes, and D. A. Lowther, *In vitro* response of chondrocytes to mechanical loading: the effect of short term mechanical tension, *Connective Tissue Res.*, **12**, 97–109 (1984).
18. R. C. Lee, J. B. Rich, K. M. Kelley, D. S. Weiman, and M. B. Mathews, A comparison of *in vitro* cellular responses to mechanical and electrical stimulations, *Am. Surg.*, **48**, 567–574 (1982).
19. G. P. J. Van Kampen, J. P. Veldhuijzen, R. Kuijter, R. J. Van de Stadt, and C. A. Schipper, Cartilage response to mechanical forces in high density chondrocytes culture, *Arth. Rheum.*, **28**, 419–424 (1985).
20. J. P. Veldhuijzen, A. H. Huisman, J. P. W. Vermeiden, and B. Prah-Andersen, The growth of cartilage cells *in vitro* and the effect of intermittent compressive force: A histological evaluation, *Connective Tissue Res.*, **16**, 187–196 (1987).
21. S. J. Milward Sadler, M. O. Wright, L. W. Davies, G. Nuki, and D. M. Salter, Mechanotransduction via integrins and IL-4 results in altered aggrecan and matrix metalloproteinase 3 gene expressions in normal, but not osteoarthritic, human articular chondrocytes, *Arthritis Rheum.*, **43**, 2091–2099 (2000).
22. J. J. Parkinnen, M. J. Lammi, S. Karjalainen, J. Laakkonen, E. Hyvarrinen, A. Thihonen, H. J. Helminen, and M. Tammi, A mechanical apparatus with microprocessor controlled stress profile for cyclic compression of cultured articular cartilage explants, *J. Biomech.*, **22**, 1285–1291 (1989).
23. G. A. Ateshian, and C. T. Hung, Functional properties of native articular cartilage. In *Functional tissue engineering* (F. Guilak and D. Butler, eds), Springer (2003).
24. J. P. G. Urban, The chondrocyte: a cell under pressure, *Brit. J. Rheumatol.*, **33**, 901–908 (1994).
25. A. M. Loening, I. E. James, M. E. Levenston, A. M. Badger, E. H. Frank, B. Kurz, M. E. Nuttal, H. H. Hung, S. M. Blake, A. J. Grodzinsky, and M. W. Lark, Injurious mechanical compression of bovine articular cartilage induces chondrocyte apoptosis, *Arch. Biochem. Biophys.*, **381**, 205–212 (2000).
26. D. D. D’Lima, S. Hashimoto, and P. C. Chen, Hydrostatic of mechanical trauma on matrix and cells, *Clin. Orthop.*, **391S**, S90–S99 (2001).
27. A. C. Hall, Differential effects of hydrostatic pressure on cation transport pathways of isolated chondrocytes, *J. Cell Physiol.*, **178**, 197–204 (1999).
28. R. L. Smith, J. Lin, M. C. D. Trindade, J. Shida, G. Kajiyama, T. Vu, A. R. Hoffman, M. C. H. van der Meulen, S. B. Goodman, D. J. Schurman, and D. R. Carter, Time-dependent effects of intermittent hydrostatic pressure on articular chondrocyte type II collagen and aggrecan mRNA expression, *J. Rehab. Res. Dev.*, **37**, 153–162 (2000).
29. L. Lipiello, C. Kaye, T. Neumata, and H. J. Mankin, *In vitro* metabolic response of articular cartilage segments to low level of hydrostatic pressure, *Connective Tissue Res.*, **13**, 99–107 (1985).
30. H. J. Hauselmann, K. Masuda, and E. B. Hunziker, Adult human chondrocytes cultured in alginate forms a matrix similar to native human articular cartilage, *Am. J. Physiol.*, **271**, 741–752 (1996).
31. K. E. Kuettner, B. U. Pauli, G. Gall, V. A. Memoli, and R. K. Schenk, Synthesis of cartilage matrix by mammalian chondrocytes culture *in vitro*. Isolation, culture characteristics and morphology, *J. Cell Biol.*, **93**, 743–750 (1982).
32. J. Guo, G. W. Jourdan, and D. K. Mccallum, Culture and growth characteristics of chondrocytes encapsulated in alginate beads, *Connective Tissue Res.*, **19**, 277–297 (1989).
33. J. D. Szafranskiy, A. J. Grodzinsky, E. Burger, V. Gaschen, H. H. Hung, and E. B. Hunziker, Chondrocyte mechanotransduction: effects of compression on deformation of intracellular organelles and relevance to cellular biosynthesis, *Osteoarthritis Cartilage*, **12**, 937–946 (2004).
34. M. J. Palmoski, and K. D. Brandt, Effect of static and compressive loading on articular cartilage plugs *in vitro*, *Arth. Rheum.*, **27**, 675–681 (1984).
35. J. K. Suh, G. H. Baek, A. Aroen, C. M. Malin, C. Niyibizi, C. H. Evans, and A. W. Larson, Intermittent sub-ambient interstitial hydrostatic pressure as a potential mechanical stimulator for chondrocyte metabolism, *Osteoarthritis Cartilage*, **7**, 71–80 (1999).

## Appendix

### *Calculation of hydrostatic pressure generated at the alginate-bound chondrocytes*

Following are the eccentricity ( $s$ ), velocity ( $v$ ) and acceleration ( $a$ ) equations of the follower:

$$\text{Eccentricity } s(\mathbf{q}) = a(1 - \cos \mathbf{q}) \quad (1)$$

$$\text{Velocity } v(\mathbf{q}) = a\mathbf{w} \sin \mathbf{q}, \quad (2)$$

$$\text{Acceleration } a(\mathbf{q}) = a\mathbf{w}^2 \cos \mathbf{q}, \quad (3)$$

where  $a$  is the linear displacement of cam (in meter) and  $\mathbf{w}$ , the angular velocity (40 rpm).

Considering the damping ratio of spring  $y = 0.10$

$$\text{Damping coefficient} \quad C = 2y m_f K \quad (4)$$

where  $m_f$  is the total mass of the follower (0.226 kg) and  $K$ , the spring constant (N/m) and

$$K = \frac{GD^4}{128R^3n} \quad (5)$$

where  $G$  = Shear modulus of spring,  $G = E/2(1 + 2\mathbf{n})$ , where  $E$  = modulus of elasticity for spring  $2.1 \times 10^{11}$  N/m<sup>2</sup>, and  $\mathbf{n}$  = Poisson's ratio (0.3).

Whereas the spring wire diameter = 1.59 mm ( $d$ ) the mean diameter of coil = 16.08 mm ( $R$ ) and the no. of turns in spring = 13 ( $n$ ). Putting the values in eqn (3) and (5),  $C = 0.74$  and  $K = \sim 61$  N/m, the force generated by loading unit on chondrocyte in one cycle can be calculated as:

$$F_c(\mathbf{q}) = m_f a(\mathbf{q}) + Cv(\mathbf{q}) + Ks(\mathbf{q}), \quad (6)$$

where  $F_c(\mathbf{q})$  is the net force at angle  $\mathbf{q}$ , keeping the values of  $a$ ,  $v$  and  $s$  from eqns (1)–(3) at various angles, the net force can be calculated at a particular angular position of the cam.

Pressure can be calculated by using the surface area of the piston ( $r = 5$  mm,  $h = 135$  mm).